PHY6011 | SOLAR CELL LABORATORY

A-site Mixed Cation Pb-based Perovskites for Stable and Efficient Photovoltaics

Submitted: 01 March 2024

Dinesh Behera[a)]

AFFILIATIONS

Department of Physics and Astronomy, The University of Sheffield, S3 7RH, United Kingdom

[a)]**Author to whom correspondence should be addressed:** dbehera1@sheffield.ac.uk

ABSTRACT

In the face of alarming global warming, the imperative for low-carbon energy technologies, particularly photovoltaics, has become even more urgent. The R&D of solar cell technologies that are not only efficient but also stable and cost-effective has emerged as a critical priority. This study investigates the optoelectronic properties and stability of perovskites, focusing on three key compositions: mono-cation MAPI, double-cation CsFAPI, and triple-cation CsFAMAPI compositions. Employing UV-vis and PL spectrophotometry, alongside low-temperature PL studies, distinct temperature-dependent trends have been learned. CsFAMAPI demonstrates superior defect tolerance and photostability compared to mono- and double-cation counterparts, with comparable phase stability to MAPI. In terms of PCE, the potential of triple-cation perovskites, reaching around 23%, outperforming MAPI (22.4%) and CsFAPI (19%) is immense. The study emphasizes the ongoing need for research in phase-stable compositions and device-specific optimization to fully harness the potential of triple-cation perovskite solar cells. These findings hold promise for advancing technologies with enhanced stability and efficiency.

I. INTRODUCTION

In photovoltaics, the ongoing research concentrates on fine-tuning the performance triangle, encompassing power conversion efficiency (PCE), stability, and production cost. Perovskites, characterised by their ABX_3 crystal structure, exhibit significant promise in solar cell devices due to their broad range tunable bandgap, high absorption coefficient, cost-effective solution-based fabrication, high efficiency, high tolerance to defects, high specific power (23 $W*g^{-1}$), and exceptional radiation tolerance.[1–4] These appealing attributes position perovskites as attractive solar cell absorbers not only for terrestrial applications but also for space applications. Selecting and combining these specific components — A = (Cs, methylammonium

(MA) or formamidinium (FA)), B = (Sn or Pb), and X = (I, Br or Cl) — influences electronic properties and stability of the perovskite absorber, including the bandgap which can be finely tuned across a range from 1.2 eV to 3.5 eV.[4]

The variations in the size of the A-site cation can noticeably influence the lattice structure. The subsequent size of the B-X bond is also a critical factor affecting the bandgap and stability of perovskite solar cells. Hence, adjusting the ratios of A-site cations in the perovskite can alter crystal properties. The suitability of an A-site cation in lead-based perovskites is evaluated through the tolerance factor (t), determined by the ionic radii of the cation (r_A), lead atom (r_{Pb}), and halide (r_X), given as $\mathbf{t = (r_A+r_X)/\sqrt{2}(r_{Pb}+r_X)}$. Varying cation sizes may induce distortion and tilt in lead halide octahedra. Significant tilting can shift the perovskite crystal phase into an undesirable phase for photovoltaic applications. A tolerance factor of 1 indicates a cubic perovskite phase, while values between 0.7 and 0.9 indicate tetragonal or orthorhombic phases.[4,5]

The conventional perovskite, $MAPbI_3$, often abbreviated as MAPI, emerged as a prominent perovskite composition due to its favorable optical and electronic properties. The use of MAPI in solar cells gained attention in the early 2010s. In a short period of a decade, the PCE surpassed 20%, making perovskite solar cells competitive with established solar cell technologies.[6,7] While MAPI showed great promise, challenges related to stability emerged. The material is sensitive to moisture and can degrade over time. Researchers are focused on addressing stability issues through material engineering and encapsulation techniques. MAPI is tetragonal at room temperature and encounters challenges such as a structural phase transition beyond 55 °C and rapid degradation in the presence of moisture, heat, and air exceeding 85 °C.[8]

In contrast, $FAPbI_3$ (FAPI) exhibits enhanced light-harvesting performance with its lower bandgap, improved thermal stability, and relatively high photostability. However, FAPI suffers structural instability at room temperature, transitioning to an undesirable non-perovskite phase in the presence of oxygen and moisture. Addressing these concerns, mixed cation and halide systems have been proposed, aiming to enhance stability. Incorporating smaller Cs ions into FA-based perovskites has proven effective in significantly improving light and moisture stability.[9–11] Perovskites can be categorized based on the quantity of A-site cations within the crystal lattice, distinguishing between mono, double, triple, and quadruple A-cation perovskites. Combining MA and FA cations can lead to a tolerance factor close to 1, contributing to enhanced stability and reduced decomposition in the presence of external factors such as humidity. Research by Saliba et al. suggests that the introduction of Cs^+ into MA/FA mixed cation perovskites can enhance phase stability, resulting in a notable 21% PCE in triple-cation perovskite solar cells.[12] To achieve long-term stability and commercial viability, ongoing research focuses on optimizing the ratios of mixed perovskites and investigating the performance of Cs-containing mixed perovskite solar cells. These endeavors aim to pave the way for the potential commercialization of perovskite solar cells.

In this research endeavor, a detailed comparative study was undertaken to assess

the properties of perovskite films, specifically focusing on three distinct compositions: mono-cation MAPI, double-cation $Cs_xFA_{1-x}PI$ (CsFAPI), and triple-cation $Cs_xFA_yMA_{1-x-y}PI$ (CsFAMAPI). The investigation encompassed a thorough examination of their absorbance characteristics and room-temperature photoluminescence responses. To delve deeper into the understanding of the phase stability exhibited by CsFAMAPI, a dedicated low-temperature photoluminescence study was also conducted. This multifaceted analysis not only sheds light on the optical behaviors of these perovskite materials but also provides crucial insights into their phase stability at different temperature regimes. The findings from this comprehensive study contribute to advancing our understanding of the optoelectronic properties of perovskites and their performance optimization through compositional engineering for various optoelectronic devices.

II. RESULTS AND DISCUSSION

A. Characterisation Setup

Following the preparation and spin-coat deposition of the perovskite films of MAPI, CsFAPI, and CsFAMAPI on glass substrates, to gain insights into the optoelectronic properties of the perovskites, UV-visible spectroscopy along with photoluminescence spectroscopy were performed, which are one of the simplest, direct, and non-destructive materials characterisation techniques to gain insights into the band structure of semiconducting materials and determine their optical bandgaps. The PL spectroscopic technique, beyond its capability to determine the optical bandgap, provides critical insights into detecting impurities and defects, particularly at lower temperatures. Consequently, it allows for the assessment of non-radiative recombination processes, making it an indispensable tool for material characterization in various applications, including photovoltaics. Furthermore, this technique is also used to measure the photostability of materials.

For the UV-visible spectrophotometry part, the equipment setup, including a UV-vis lamp (DH-2000-BAL), a precisely aligned lens system on an optical bench, fiber optic cables for efficient light transfer, a high-resolution spectrometer (HR2000+ES), the OceanView data acquisition and analysis software, all from Ocean Optics, was employed. For the PL spectrophotometry, the equipment setup remained consistent, albeit with a notable modification: the UV-Vis lamp was replaced by a 405 nm class-2 laser diode (PL205) from Thorlabs. Further, the low-temperature PL studies were carried out using the dry cryostat (OptistatDry BLV) by Oxford Instruments, ensuring a controlled low-temperature environment crucial for exploring the temperature-dependent photoluminescence behaviors of the perovskite films.

B. Optoelectronic Properties

To calculate the bandgap energy (E_g) of the perovskite films using UV-visible spectroscopy, the intensity of the light incident (I_0) on and transmitted (I) from the thin films of perovskite materials is measured, and further absorbance (A) of the materials is calculated using $\mathbf{A = log_{10}(I/I_0)}$ and plotted against wavelength (in nm) as shown in FIG. 1 (a). Further, to reconfirm the bandgap and calculate the Urbach energy, the absorption coefficient (α) is calculated from the absorbance (A) using the Beer-Lambert's law,

$I/I_0 = exp(-\alpha*t)$, where t is the thickness of the material. And, using the abovementioned equation for absorbance, it further implies that the absorbance **$A = -\alpha*t*log(e)$**, and finally becomes **$\alpha = 2.303*A/t$**. For the used perovskite samples, the thickness of the films t = 400 nm, and hence it can be inferred that **$\alpha = 2.303*A/(4*10^{-5})$ cm^{-1}**. The absorption coefficient is plotted against the photon energy to determine and reconfirm the bandgap and the energetic measure of the disorders in the perovskite films (E_U) is calculated as the inverse of the slope of the curve of ln(α) vs photon energy (E) based on the equation **$\alpha = \alpha_0 \exp((E-E_g)/E_U)$**. The peaks of the PL spectra of the perovskite films further reconfirm their bandgaps as shown in FIG. 2. The bandgaps of the films were found to be 1.59 eV for MAPI, 1.55 eV for CsFAPI, and 1.60 eV for CsFAMAPI. The Urbach energies were similar for MAPI and CsFAPI being 89 meV and 96 meV respectively while that of the CsFAMAPI came out to be 62 meV. This suggests that the defect tolerance of the triple-cation perovskite is superior to that of the mono- and double-cation perovskites.

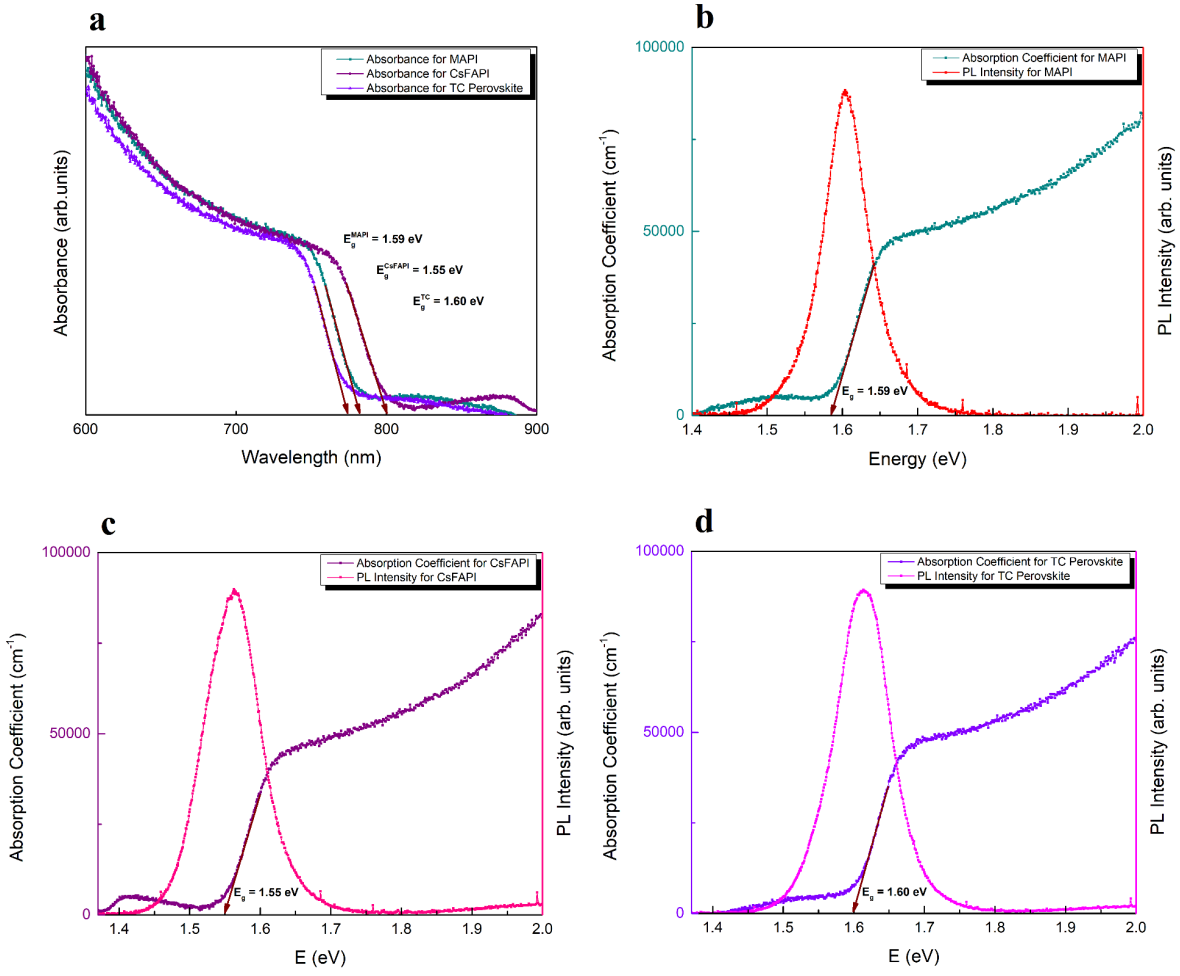

FIG. 1. (a) Absorbance spectra for the three perovskite film samples showing their bandgaps; and the absorption coefficient spectra with the PL spectra reconfirming the bandgaps of the three perovskite film samples: (b) MAPI, (c) CsFAPI, and (d) CsFAMAPI.

C. Degradation Studies

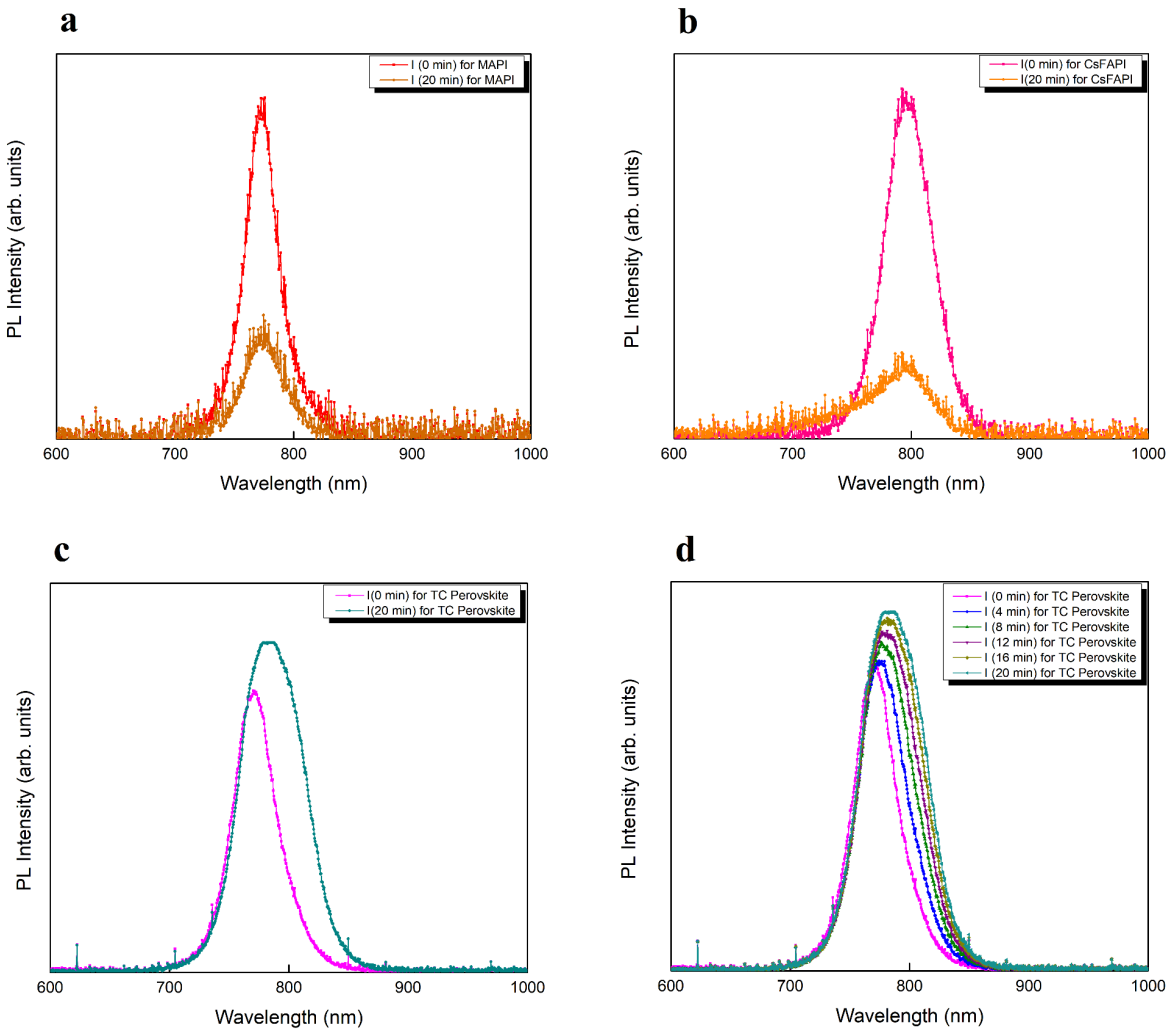

FIG. 2. PL spectra showing the degradation of perovskite film samples (a) MAPI and (b) CsFAPI, under light illumination for 20 minutes; (c) showing the photostability of the CsFAMAPI perovskite sample; further, (d) shows the changes per 4 minutes time interval for the CsFAMAPI for better clarity.

The PL spectra of the perovskite films were further studied over a period of 20 minutes each to gain insight into the degradation of the materials under continuous exposure to light. The perovskite films CsFAPI and CsFAMAPI are more efficient in terms of photoemissions over MAPI. Further, it can be seen that the perovskite films of MAPI and CsFAPI degrade and their non-radiative recombinations increase under continuous light exposure. CsFAPI shows an asymmetric PL curve after 20 mins of exposure, which indicates A-site cation phase segregation. In contrast, the CsFAMAPI shows the opposite behaviour of increasing its radiative recombinations under continuous illumination. This shows that the triple-cation perovskite is better in terms of photostability than its mono- and double-cation counterparts. To shed more light on the photostability of the triple-cation

perovskite film, a series of measurements of PL emission was conducted, spaced by equal time intervals (1 minute) over a period of 20 minutes as the films were continuously exposed to the laser. However, the PL spectral plot shows the trend for every interval of 4 minutes in FIG. 4. One can see that the PL intensity increases and the PL peak shifts with increasing time, signifying that the photoemission efficiency increases and the bandgap decreases (PL peak redshift) under continuous light exposure, which indicates the onset of A-site phase segregation.

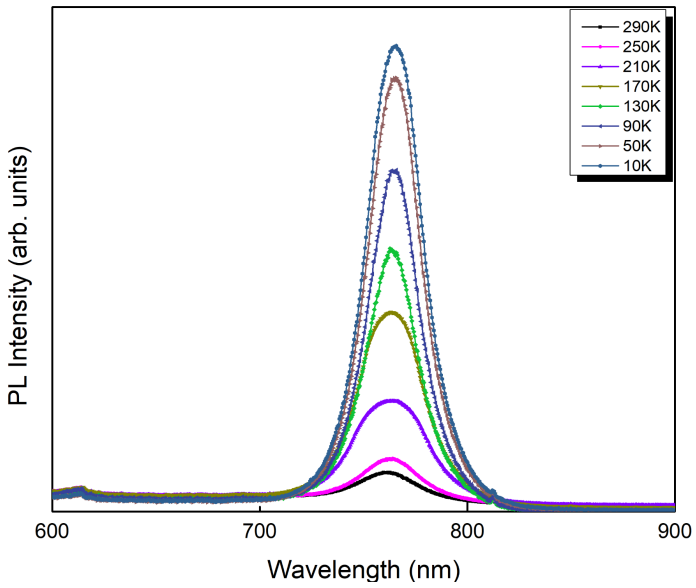

FIG. 3. Temperature-dependent PL spectra showing the changes in the PL peak per fall in 40 K going from 290 K to 10 K.

Furthermore, a temperature-dependent PL study was carried out for the phase stability triple-cation perovskite film sample. In this study, the PL spectra of the triple-cation perovskite were plotted for every fall in 10 K of sample temperature from 293 K to 10 K. Here, however, in the FIG. 3., the spectral plots considered are from 290 K to 10 K for every 40 K. The spectral plots show that the photoemission efficiency increases with decreasing the sample temperature, which is due to the bound-excitons not getting enough thermal energy to dissociate and reach the defects-mediated non-radiative recombination centres and consequentially recombining radiatively. Further, as the temperature decreases, the PL peaks experience a reduction in width. This narrowing phenomenon is attributed to the diminishing presence of phonons, leading to a decreased homogeneity in the broadening of the PL signal caused by exciton-phonon coupling.[13,14] To study this phenomenon quantitatively, the peak positions (signifying the optical bandgaps) of the temperature-dependent PL spectra were recorded against temperature and plotted in FIG. 7. It can be seen that the triple-cation perovskite maintains its tetragonal phase till 190 K and transitions into orthorhombic phase at temperatures lower than 190K. For MAPI, the phase transition takes place at 160 K,[15,16] implying that the tetragonal phase of MAPI is more stable than that of CsFAMAPI, which can be due to the

complexities in terms of unstable compositions of Cs/FA/MA in the triple-cation perovskite.[17] To make it more clear, the bandgap (denoted by the wavelength of the peak of the PL signal) of the triple-cation perovskite changes from 1.607 to 1.600 eV on reducing the sample temperatures from 290 to 10 K, which is in agreement with the Varshini effect, which establishes the bandgap of a material as a function of temperature.[18]

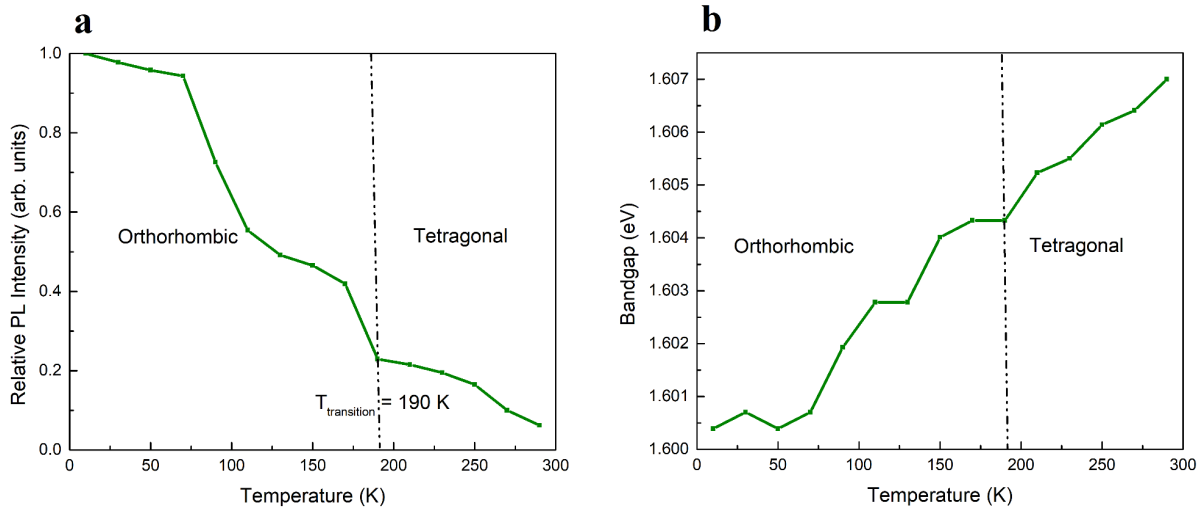

FIG. 4. (a) The normalised PL peak intensity is plotted against the temperature for the sample of CsFAMAPI, showing a phase transition at 190 K; and (b) shows the bandgap of CsFAMAPI plotted against the temperature, reconfirming the phase transition at 190 K.

III. CONCLUSION

In conclusion, this investigation into the optoelectronic properties of perovskite films, including mono-cation MAPI, double-cation CsFAPI, and triple-cation CsFAMAPI, has provided valuable insights into their behavior using the UV-visible and photoluminescence spectrophotometry analyses, along with low-temperature PL studies, revealed distinct temperature-dependent trends. Further, it can be established that the triple-cation perovskite is better than mono- and double-cation perovskites in terms of defect tolerance and photostability, and is comparable in terms of phase stability to MAPI. In terms of PCEs, triple-cation perovskites have reached around 23% while the MAPI and CsFAPI perovskites have reached about 22.4% and 19% respectively.[19–21] MAPI, CsFAPI, and CsFAMAPI perovskites have the potential to attain realistic PCEs of 24%, 23%, and 28% as suggested by Martin Stolterfoht et al.[22] However, unlocking the full potential of triple-cation perovskite solar cells requires meticulous research in terms of phase-stable compositions to reduce cation phase segregation and also device-specific research which includes optimizing PCEs by additive engineering and interfacial defect passivation. Continued research in this direction holds promise for advancing the development of triple-cation perovskite-based solar cell technologies with enhanced stability and efficiency.

ACKNOWLEDGEMENTS

The author would like to express their sincere gratitude to Prof. David Lidzey and Dr. Alex Ramadan for their invaluable support and supervision during the Solar Cell Laboratory

course module of the MSc in Solar Cell Technology programme (2023-24) at the Department of Physics and Astronomy, The University of Sheffield. Their guidance and expertise have been instrumental in the successful completion of this work. The author also acknowledges the Department of Physics and Astronomy for providing the necessary resources and facilities for conducting the research.

DATA AVAILABILITY

The data that support the findings of this study are available from the corresponding author upon reasonable request.

REFERENCES

[1] G.E. Eperon, M.T. Hörantner, and H.J. Snaith, "Metal halide perovskite tandem and multiple-junction photovoltaics," Nat. Rev. Chem. **1**(12), 1–18 (2017).

[2] Y. Tu, J. Wu, G. Xu, X. Yang, R. Cai, Q. Gong, R. Zhu, and W. Huang, "Perovskite Solar Cells for Space Applications: Progress and Challenges," Adv. Mater. **33**(21), 2006545 (2021).

[3] F. Lang, G.E. Eperon, K. Frohna, E.M. Tennyson, A. Al-Ashouri, G. Kourkafas, J. Bundesmann, A. Denker, K.G. West, L.C. Hirst, H.-C. Neitzert, and S.D. Stranks, "Proton-Radiation Tolerant All-Perovskite Multijunction Solar Cells," Adv. Energy Mater. **11**(41), 2102246 (2021).

[4] J. Albero, A. M. Asiri, and H. García, "Influence of the composition of hybrid perovskites on their performance in solar cells," J. Mater. Chem. A **4**(12), 4353–4364 (2016).

[5] R. Prasanna, A. Gold-Parker, T. Leijtens, B. Conings, A. Babayigit, H.-G. Boyen, M.F. Toney, and M.D. McGehee, "Band Gap Tuning via Lattice Contraction and Octahedral Tilting in Perovskite Materials for Photovoltaics," J. Am. Chem. Soc. **139**(32), 11117–11124 (2017).

[6] Z. Chen, B. Turedi, A.Y. Alsalloum, C. Yang, X. Zheng, I. Gereige, A. AlSaggaf, O.F. Mohammed, and O.M. Bakr, "Single-Crystal MAPbI3 Perovskite Solar Cells Exceeding 21% Power Conversion Efficiency," ACS Energy Lett. **4**(6), 1258–1259 (2019).

[7] H.J. Snaith, "Present status and future prospects of perovskite photovoltaics," Nat. Mater. **17**(5), 372–376 (2018).

[8] B. Conings, J. Drijkoningen, N. Gauquelin, A. Babayigit, J. D'Haen, L. D'Olieslaeger, A. Ethirajan, J. Verbeeck, J. Manca, E. Mosconi, F.D. Angelis, and H.-G. Boyen, "Intrinsic Thermal Instability of Methylammonium Lead Trihalide Perovskite," Adv. Energy Mater. **5**(15), 1500477 (2015).

[9] D.-H. Choi, H.-J. Seok, S.-K. Kim, D.-H. Kim, B. Hou, and H.-K. Kim, "The Effect of Cs/FA Ratio on the Long-Term Stability of Mixed Cation Perovskite Solar Cells," Sol. RRL **5**(12), 2100660 (2021).

[10] M.M. Byranvand, C. Otero-Martínez, J. Ye, W. Zuo, L. Manna, M. Saliba, R.L.Z. Hoye, and L. Polavarapu, "Recent Progress in Mixed A-Site Cation Halide Perovskite Thin-Films and Nanocrystals for Solar Cells and Light-Emitting Diodes," Adv. Opt. Mater. **10**(14), 2200423 (2022).

[11] G.E. Eperon, S.D. Stranks, C. Menelaou, M.B. Johnston, L.M. Herz, and H.J. Snaith, "Formamidinium lead trihalide: a broadly tunable perovskite for efficient planar heterojunction solar cells," Energy Environ. Sci. **7**(3), 982–988 (2014).

[12] M. Saliba, T. Matsui, J.-Y. Seo, K. Domanski, J.-P. Correa-Baena, M.K. Nazeeruddin, S.M. Zakeeruddin, W. Tress, A. Abate, A. Hagfeldt, and M. Grätzel, "Cesium-containing triple cation perovskite

solar cells: improved stability, reproducibility and high efficiency," Energy Environ. Sci. **9**(6), 1989–1997 (2016).

[13] C. Wehrenfennig, M. Liu, H.J. Snaith, M.B. Johnston, and L.M. Herz, "Charge carrier recombination channels in the low-temperature phase of organic-inorganic lead halide perovskite thin films," APL Mater. **2**(8), 081513 (2014).

[14] R.L. Milot, G.E. Eperon, H.J. Snaith, M.B. Johnston, and L.M. Herz, "Temperature-Dependent Charge-Carrier Dynamics in CH3NH3PbI3 Perovskite Thin Films," Adv. Funct. Mater. **25**(39), 6218–6227 (2015).

[15] O. Plantevin, S. Valère, D. Guerfa, F. Lédée, G. Trippé-Allard, D. Garrot, and E. Deleporte, "Photoluminescence Tuning Through Irradiation Defects in CH3NH3PbI3 Perovskites," Phys. Status Solidi B **256**(10), 1900199 (2019).

[16] B.J. Foley, D.L. Marlowe, K. Sun, W.A. Saidi, L. Scudiero, M.C. Gupta, and J.J. Choi, "Temperature dependent energy levels of methylammonium lead iodide perovskite," Appl. Phys. Lett. **106**(24), 243904 (2015).

[17] L. Liu, J. Lu, H. Wang, Z. Cui, G. Giorgi, Y. Bai, and Q. Chen, "A-site phase segregation in mixed cation perovskite," Mater. Rep. Energy **1**(4), 100064 (2021).

[18] Y.P. Varshni, "Temperature dependence of the energy gap in semiconductors," Physica **34**(1), 149–154 (1967).

[19] X. Tian, S. Zhang, Z. Shen, B. Zhang, Y. Hong, R. Liu, Y. Liu, R. Cao, J. Song, H. Li, F. Li, and C. Chen, "Functional 1,3-DTu Additive in Perovskite Layer for Stable Triple-Cation Perovskite Solar Cells with Efficiency Exceeding 23%," Sol. RRL **8**(1), 2300810 (2024).

[20] W. Qiu, Y. Wu, Y. Wang, Z. Yang, R. Yang, C. Zhang, Y. Hao, and Y. Hao, "Low-Temperature robust MAPbI3 perovskite solar cells with power conversion efficiency exceeding 22.4%," Chem. Eng. J. **468**, 143656 (2023).

[21] T. Thornber, O.S. Game, E.J. Cassella, M.E. O'Kane, J.E. Bishop, T.J. Routledge, T.I. Alanazi, M. Togay, P.J.M. Isherwood, L.C. Infante-Ortega, D.B. Hammond, J.M. Walls, and D.G. Lidzey, "Nonplanar Spray-Coated Perovskite Solar Cells," ACS Appl. Mater. Interfaces **14**(33), 37587–37594 (2022).

[22] M. Stolterfoht, M. Grischek, P. Caprioglio, C.M. Wolff, E. Gutierrez-Partida, F. Peña-Camargo, D. Rothhardt, S. Zhang, M. Raoufi, J. Wolansky, M. Abdi-Jalebi, S.D. Stranks, S. Albrecht, T. Kirchartz, and D. Neher, "How To Quantify the Efficiency Potential of Neat Perovskite Films: Perovskite Semiconductors with an Implied Efficiency Exceeding 28%," Adv. Mater. **32**(17), 2000080 (2020).